POLİTEKNİK DERGİSİ

JOURNAL of POLYTECHNIC

ISSN: 1302-0900 (PRINT), ISSN: 2147-9429 (ONLINE)
URL: http://dergipark.org.tr/politeknik

Adiabat shaping in direct drive ınertial confinement fusion ımplosions through the decaying shock approximation

Doğrudan tahrikli eylemsiz hapsedilme füzyon içersinde azalan şok yaklaşımı boyunca adiabat şekillendirme

***Yazar(lar) (Author(s))**: Samira MOHAMMADKHANI[1], Abbas GHASEMIZAD[2]*

ORCID[1]: 0000-0003-4356-7229

ORCID[2]: 0000-0001-6452-6309

Bu makaleye şu şekilde atıfta bulunabilirsiniz(To cite to this article): Mohammadkhani S. and Ghasemizad A., "Adiabat shaping in direct drive ınertial confinement fusion ımplosions through the decaying shock approximation", ***Politeknik Dergisi***, 24(3): 1063-1072, (2021).

Erişim linki (To link to this article): http://dergipark.org.tr/politeknik/archive

DOI: **10.2339/politeknik.806704**

Adiabat Shaping in Direct Drive Inertial Confinement Fusion Implosions through the Decaying Shock Approximation

Highlights

- *The implosions of a double-layer spherical target driven by a two-step pressure pulse is considered.*
- *The adiabat of the entropy is shaped by employing the Decaying Shock method.*
- *The optimum adiabat parameter is calculated for three different fuel density states.*
- *The effect of the initial density on the adiabat parameter is obtained.*

Graphical Abstract

In this study we have considered the implosions of a two-layer spherical shell, one of which consists of DT fuel and the other acts like a pusher layer, accelerated by the shock waves generated by a two-step pressure pulse.

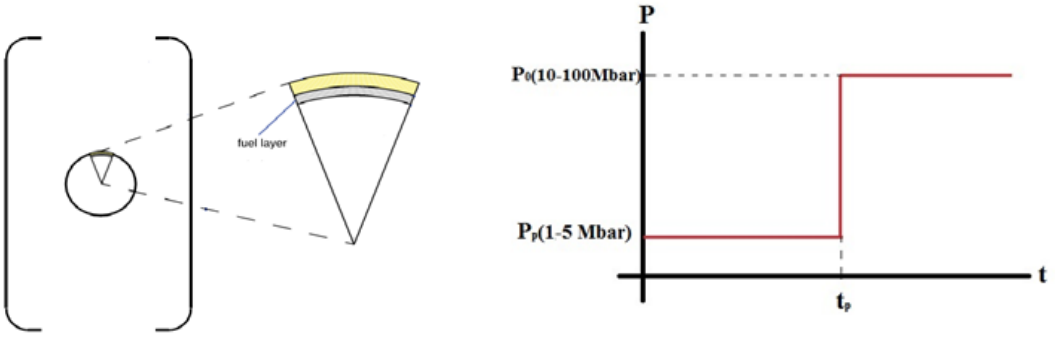

Figure

Aim

The aim of the present study is the investigation of the shaping the adiabat of the entropy in Inertial Confinement Fusion (ICF) implosions.

Design & Methodology

The adiabat is shaped by the Decaying Shock (DS) method and the optimum adiabat parameter is calculated for three different fuel density states.

Originality

The DS-shaped adiabat follows a power law in agreement with the established theoretical models. The obtained adiabat values are found comparable with those in previous investigations, although they are achieved for relatively faster irradiation times and lower laser intensities.

Findings

It is found that the higher the initial density is, the lower adiabat parameter.

Conclusion

Shaping the adiabat of the entropy during the implosions of ICF capsules plays an important role in the control and efficiency of the fuel targets in relation to a balance between energy gaining and stability.

Declaration of Ethical Standards

The author(s) of this article declare that the materials and methods used in this study do not require ethical committee permission and/or legal-special permission.

Adiabat Shaping in Direct Drive Inertial Confinement Fusion Implosions through the Decaying Shock Approximation

Araştırma Makalesi / Research Article

Samira MOHAMMADKHANI[1], Abbas GHASEMIZAD[2*]

[1] Department of Physics, University campus 2, University of Guilan, Rasht, Iran
[2] Department of Physics, Faculty of Science, University of Guilan, P.O. Box 1914, Rasht, Iran

(Geliş/Received : 06.10.2020 ; Kabul/Accepted : 19.11.2020 ; Erken Görünüm/Early View : 15.12.2020)

ABSTRACT

We consider the implosions of a double-layer spherical target driven by a two-step pressure pulse. By employing the decaying shock approximation the adiabat of the entropy is shaped, following a simple power law in agreement with the established theoretical models. Then we directly calculate the optimum adiabat parameter for three different fuel density states and find that the higher the initial density is, the lower adiabat parameter. Although the calculated adiabat values are close to ones obtained in previous investigations, they are achieved for relatively fast irradiation times and low laser intensity.

Keywords: Inertial confinement fusion, adiabat shaping, decaying shock method.

Doğrudan Tahrikli Eylemsiz Hapsedilme Füzyon içersinde Azalan Şok Yaklaşımı Boyunca Adiabat Şekillendirme

ÖZ

Bu çalışmada, iki aşamalı bir basınç darbesi ile tahrik edilen çift katmanlı küresel bir hedefin iç patlamalarını inceledik. Çalışmada ilk önce azalan şok yaklaşımı kullanılarak entropinin adiabatının, yerleşik teorik modellerle uyumlu basit bir güç yasasını izleyerek nasıl bir forma dönüştüğünü belirledik. Daha sonra üç farklı yakıt yoğunluğu koşulu için optimum adiabat parametresini doğrudan matematiksel yaklaşımla ,başlangıç yoğunluğu ne kadar yüksekse ve adiabat parametresinin bir o kadar azaldığını hesapladık. Sonuç olarak, nispeten hızlı ışınlama süreleri ve düşük lazer yoğunluğu için, tabakalı adiyabitik değerlerimizin literatürdeki çalışmalarla uyumlu olduğunu belirledik.

Anahtar Kelimeler: Eylemsiz füzyon hapsetme, adiabat şekillendirme, azalan şok yaklaşımı.

1. INTRODUCTION

In inertial confinement fusion (ICF) approach [1, 2] the energy produced by lasers is deposited into the outer surface of a small spherical shell of fusible fuel ionizing a part of its outer material. Thermal energy is transferred inward up to an ablation surface which separates the hot plasma from the inner dense part of the shell, forcing the plasma to blast outwards by a rocket-like blow-off. Reaction forces create inward-traveling shock waves that compress the core of the pellet causing it to implode, thus, creating the appropriate conditions for ignition to take place. In direct drive ICF [3–5] the compression of the target is based on its uniform bombardment by symmetrically placed laser beams directly onto the shell's surface. The target, which ideally has to be perfectly symmetric, is composed by a layer filled with cryogenic solid deuterium-tritium (DT) fuel deposited in an outer layer of ablator material that acts like a pusher; the inner part of the pellet usually consists of a layer filled with DT gas and is in thermal equilibrium with the dense, solid DT fuel.

The aforementioned process is susceptible to the Rayleigh-Taylor (RT) instability [6, 7] which occurs due to the local created density gradients between the inner and the outer parts of the shell material; controlling the growth of the RT instability is crucial to the success of the process [8]. The hydrodynamic instability is seeded by imperfections in target design as well as by laser non-uniformities (laser imprint), leading to modulations on both the ablation and the inner shell surfaces. However, phenomena like mass ablation and thermal transport are found to reduce the instability growth rates and play a stabilizing role in shorter wavelengths [9–12].

An important parameter in ICF hydrodynamic theory is the adiabat α, defined as the ratio of the shell pressure, P, to the Fermi-degenerate pressure calculated at the shell density, through $\alpha \equiv P/\left(2.18\rho^{5/3}\right)$, where the pressure is measured in Mb and density measured in g/cm^3. Adiabat shaping [13–16] has the potential to achieve optimum balance between improved stability and high

*Sorumlu Yazar (Corresponding Author)
e-posta : ghasemi@guilan.ac.ir

target gain [17–20]. In standard direct drive laser implosions laser beams generate shaped pressure pulses that drive multiple shock-waves capable of compressing the target and shaping the adiabat. In practice, a strong shock launched from the picket pulse which later decays as it propagates through the shell, on the one hand raises the ablation velocity and therefore the adiabat value on the ablation surface, while on the other hand establishes the adiabat of the inner surface at a low value. It follows that for a shaped driver pressure, the increase in the entropy becomes smaller as the density increases, and therefore, the adiabat parameter can also be interpreted as a measure of the deviation from the minimum energy required to compress the fuel for which minimum entropy is added; since a low entropy fuel is easier to compress, the compression must approximately be isentropic. The relations for the pressure and density of an ideal fuel in terms of the radius, for each pulse being fired towards the center of the sphere during such an isentropic compression of a two-layer shell driven by a two-step pressure pulse, were obtained in [21].

At least two different techniques have been proposed for adiabat shaping in direct drive implosions; these are the decaying shock (DS) method [13,14] and the relaxation (RX) method [15,16]. In the DS approximation a strong shock launched by the prepulse is used to shape the adiabat after it later starts decaying when propagating into the inner shell material as the prepulse is switched off; on the other hand in the RX method the adiabat is shaped by the main strong shock, after the pressure and density profiles are relaxed by the prepulse decaying shock. It was found that a DS-shaped adiabat follows a power law with respect to the mass [14], as

$$\alpha = \alpha_{inn}\left(\frac{m}{m_s}\right)^{\delta}, \qquad (1)$$

where m denotes the mass coordinate calculated from the outer surface, m_s is the total areal mass of the capsule and α_{inn} corresponds to the adiabat parameter on the inner surface; the exponent δ is approximately independent of the initial pulse characteristics. The effect of such steep adiabat profiles were investigated by two dimensional simulations in [19, 22]. In general, shaped adiabat profiles are found to be more beneficial, with respect to improved stability, than flat ones ($\alpha \approx \alpha_{inn}$).
In this work the implosion of a two layer shell driven by a two-step pressure pulse as that introduced in Ref. [21] is considered. The DS method is employed to shape the adiabat of the entropy which follows a power law as that in (1). Specifically, in section 2 the general problem of the decaying shock for the two-layer shell presented in Ref. [21] is reviewed. The pressure and density in the shell are formulated in Hugoniot conditions together with the equations of motion, once first obtained in terms of the surface mass. In section 3 the pertinent differential equations are solved approximately by employing the Decaying Shock method, and the applied pressure, pulse radiation time, laser intensity and adiabat parameter are directly calculated for three different states considered. We find that the optimum state with respect to the minimum adiabat parameter corresponds to shell's initial density equal to 0.6 g/cm^3, and post shock density equal to 2.4 g/cm^3, achieved in relatively fast pulse radiation times. Finally, Section 4 summarizes the main results.

2. IMPLOSIONS OF A DOUBLE-LAYER TARGET

2.1 Pressure and Density in a Spherical Shell

We consider a small spherical shell consisting of an outer pusher layer of ablative material and an inner solid cryogenic DT fuel layer, followed by a vacuum layer, as shown in Fig. 1.

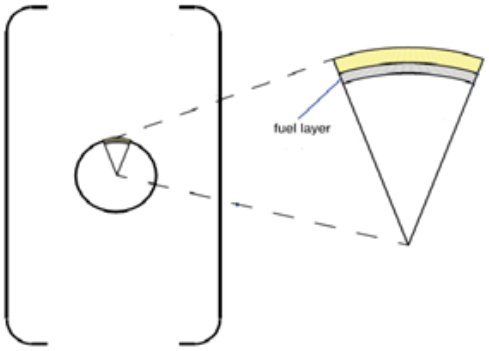

Figure 1. Schematic of a two-layer spherical fuel with an empty center.

In principle, for the implosion of the target at a low isentrope, at least two shock waves are required. We study the propagation of the shock waves driven by a two-step pressure pulse directly applied to the spherical target over a time interval Δt, as that shown in Fig. 2.
At the first stage a low pressure P_p of the order of 1 to 5 Mb drives the first shock, while at the time t_p a sudden jump in the pressure P_0 of the order of 10 to 100 Mb launches the second shock wave. The applied pressures are assumed to be sufficient for the generation of strong shocks that drive the entropy in the shell. Also, all non-ideal phenomena are neglected, and therefore, both the pusher material and the fuel are treated as ideal gases with enthalpy constant $\gamma = 5/3$.

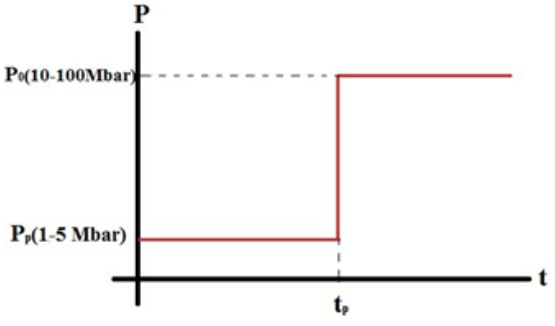

Figure 2. The pressure diagram applied in terms of time.

In the beginning of the process a shock wave is launched by the pressure prepulse at t_0, setting the pressure of the pusher to the value P_p. Expansion of the pusher results in a decrease of the radius of the target, the density of which increases, thus, converting it into plasma. This wave then propagates inside the fuel layer and when it reaches the layer-vacuum interface, at time t_1, a rarefaction shock is reflected off the vacuum boundary surface; the rarefaction shock then moves towards the ablation surface and arrives at the pusher layer at time τ_1. The pressure and density profiles in this stage where acquired via an isentropic expansion [21,23], being uniform in the regions that are not affected by the rarefaction for times $\tau < t_1$. Furthermore, at time t_p the laser-intensity is highly increased and a second shock is launched in the pusher layer due to the main pressure pulse, P_0. This shock catches up with the rarefaction one at time t_B, when the radius of shell equals R_B, and interferes with it. When it later reaches the fuel vacuum surface it shapes the pressure and density profiles as that introduced in Ref. [21], leaving the entropy profile almost uniform until the end of the implosion once additional sources of entropy generation, such as preheating due to superthermal electrons, are neglected. We note that for effectively achieving high compression of the shell precise timing between the shocks is required [24,25]. The shock-waves generation and propagation details during the aforementioned process are illustrated in Fig. 3.

The compression of the fuel must be achieved rapidly and in an isentropic manner [1]. After the vacuum space is enclosed at t_0, the velocity of the shell reduces, leading to its deceleration without significant change in the entropy. In this stage, the kinetic energy of the shell is completely trasformed into internal energy and the maximum pressure, density and temperature values are achieved at time t_m. Piriz and Wouchuk obtained the pressure and density profiles during an isentropic compression under the assumption that the velocity of the shell is small compared to the implosion velocity at times close to t_m; these are given as functions of the radius r, measuring the distance from the center, by the following relations [21]:

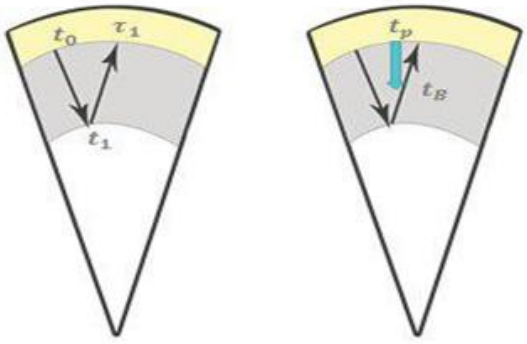

Figure 3. The position of the first wave, the wave of rarefaction, the second wave and the interference of the first and second wave at time t_B.

$$P(r) = \begin{cases} P_B\left(\frac{R_m - r}{R_m - R_B}\right)^{3\gamma/2}, & r \geqslant R_B \\ P_c\left[1 - A\left(\frac{r}{R_B}\right)^4\right]^{3\gamma/2}, & r < R_B \end{cases} \quad (2)$$

and

$$\rho(r) = \begin{cases} \left(\frac{P_B}{\sigma}\right)^{1/\gamma}\left(\frac{R_m - r}{R_m - R_B}\right)^{5/2\gamma}, & r \geqslant R_B \\ \left(\frac{P_c}{\sigma}\right)^{1/\gamma}\left(\frac{r}{R_B}\right)^3\left[1 - A\left(\frac{r}{R_B}\right)^4\right]^{5/2\gamma}, & r < R_B \end{cases} \quad (3)$$

where, $\rho_0$denotes the initial density of the shell, $\sigma = P_0/(16\rho_0)^\gamma$, $A = 1 - (P_B/P_c)^{2/5}$, $P_c = P(r = 0)$, $P_B = P(r = R_B)$ and $R_m = r(t = t_m)$. Equations (2) and (3) can be simplified in a form relating the pressure directly with the density for the two regions in the shell; this is given by

$$\rho(r) = \begin{cases} \left(\frac{P}{\sigma}\right)^{1/\gamma}\left\{\frac{1}{A}\left[1 - \left(\frac{P}{P_c}\right)^{2/3\gamma}\right]\right\}^{3/4}, & r < R_B \\ \left(\frac{P}{\sigma}\right)^{1/\gamma}, & r \geq R_B \end{cases} \quad (4)$$

implying that $P \propto \rho^\gamma$ for $r \geq R_B$. The above relations denfine the final form of the pressure and density of the second shock wave obtained for the implosions of a spherical double-layer shell, and therefore the adiabat parameter.

2.2 Dynamics of the Implosion

The dynamics of the shocked material is determined by the equations of motion for the fluid together with the Hugoniot conditions [26,27]. In one dimensional geometry, the equations governing mass, momentum and energy conservation can be interpreted in a Lagrangian frame by changing the independent spatial coordinate r with the mass areal density m, in the form [14, 15]:

$$\frac{\partial u}{\partial m} - \frac{\partial}{\partial t}\frac{1}{\rho} = 0 \quad (5)$$

$$\frac{\partial u}{\partial t} + \frac{\partial P}{\partial m} = 0 \quad (6)$$

$$\frac{\partial}{\partial t}\left(\frac{P/\rho}{\gamma - 1} + \frac{u^2}{2}\right) + \frac{\partial}{\partial m}(Pu) = 0 \quad (7)$$

where u is the velocity, ρ is the density, and P is the pressure of the fluid as functions of m and t. Note that in the adopted frame of reference the outer surface of the shell is defined by $m = 0$. The above equations refer to an ideal gas of index γ, in which phenomena related with thermal conductivity and fluid viscocity are neglected. However, plasma viscocity may have some important impact on the implosions [28]. The Hugoniot relations

are jump conditions providing the connection between the pre- and post- shock macroscopic variables of the material, and can be derived by an integration of the equations of motion at the shock front. In the strong shock regime they are given by the forms:

$$\rho_M = \frac{\gamma+1}{\gamma-1}\rho_0, \tag{8}$$

$$u_M = \frac{2}{\gamma-1}\frac{m_s}{\rho_M}, \tag{9}$$

$$\dot{m}_s = \sqrt{\frac{(r-1)}{2}P_M\rho_M}, \tag{10}$$

connecting the areal mass, m_s, with the post shock density, velocity and pressure. Here, the subscript M refers to the post shock variables, while the dot (.) implies differentiation with respect to t. Therefore, substitution of equation (4) for $\rho = \rho_M$ and $P = P_M$ into (10) yields the following expression of the time derivative of the surface mass, as a function of either the post shock density or post shock pressure in the spherical shell under consideration:

$$\dot{m}_s = \begin{cases} \sqrt{\frac{\sigma(\gamma-1)}{2}P_M^{(\gamma+1)/\gamma}\left[1-\left(\frac{P_M}{P_c}\right)^{2/3\gamma}\right]^{5/4\gamma}}, r < R_B \\ \sqrt{\frac{\sigma(\gamma-1)}{2}\rho_M^{\gamma+1}}, r \geq R_B. \end{cases} \tag{11}$$

Following Refs. [14, 15], we introduce the dimensionless variable

$$\varepsilon \equiv \frac{m}{m_s(t)} \tag{12}$$

and the following normalized macroscopic fluid variables in terms of ε

$$\rho_N(\varepsilon) = \frac{\rho}{\rho_M},\ P_N(\varepsilon) = \frac{P}{P_M},\ u_N(\varepsilon) = \frac{u}{\dot{m}_s/\rho_M} \tag{13}$$

under which the mass conservation and momentum conservation equations can be brought in dimensionless form. In specific, substituting the normalized parameters given in Eq. (13), under the appropriate relations for $\dot{m}_s$, ρ_M, and P_M, obtained in Eqs. (4)-(11), into Eqs. (5) and (6) yields a pair of coupled ODE's for each different region with respect to r. These are:

$$\begin{aligned} &\frac{du_N(\varepsilon)}{d\varepsilon} - \frac{\varepsilon}{\gamma}\frac{1}{P_N(\varepsilon)^{(\gamma+1)/\gamma}}\frac{dP_N(\varepsilon)}{d\varepsilon} = 0, \\ &\varepsilon\left(\frac{\gamma-1}{2}\right)\frac{du_N(\varepsilon)}{d\varepsilon} - \frac{dP_N(\varepsilon)}{d\varepsilon} = 0, \end{aligned} \tag{14}$$

valid for $r < R_B$, coupled through the normalized velocity and pressure, and

$$\begin{aligned} &\frac{du_N(\varepsilon)}{d\varepsilon} - \frac{\varepsilon}{\rho_N(\varepsilon)^2}\frac{d\rho_N(\varepsilon)}{d\varepsilon} = 0, \\ &\frac{\varepsilon(\gamma-1)}{2\gamma}\frac{du_N(\varepsilon)}{d\varepsilon} - \rho_N(\varepsilon)^{(\gamma-1)}\frac{d\rho_N(\varepsilon)}{d\varepsilon} = 0, \end{aligned} \tag{15}$$

valid in the region $r \geqslant R_B$, and coupled through the normalized velocity and density functions. For a well posed solution the above equations must be solved with appropriate boundary conditions; these are given by the Hugoniot relations at the shock front as

$$\rho_N(\varepsilon = 1) = 1, u_N(\varepsilon = 1) = \frac{2}{\gamma-1}. \tag{16}$$

Adiabat shaping relies on the solution of the above equations once the pressure and density profiles are determined.

In Ref. [15] an isentropic flow condition was considered; in the absence of shocks the energy equation reduces to $P = S(m)\rho^\gamma$, where S is the adiabat shaping of the entropy for the specific process and which depends only on the coordinate m. We further consider the case $r \geqslant R_B$ assuming that $P_N = \rho_N^\gamma$. The schock wave launched by the strong pressure pulse sets the shocked material to a constant adiabat value, $S(m) = \frac{P}{\rho^\gamma} = \frac{P_M}{\rho_M^\gamma} = \sigma = const.$, as follows from relations (4), $P_M = \sigma\rho_M^\gamma$. Thus, the post shock pressure and density through the solution of the pertinent system of differential equation (15) determine the shape of the adiabat, which we have found to be constant. However, such a state is ideal and impossible to achieve in ICF fusion related experiments, since for a constant adiabat value the applied pressure should not depend on time. Owing to the Hugoniot conditions, a simple integration of the momentum conservation equation yields

$$P(m=0,t) = \sqrt{\frac{\gamma-1}{2}\frac{P_0}{(16\rho_0)^\gamma}}\rho_M^{(\gamma+1)/2}\int_0^1 u d\varepsilon, \tag{17}$$

and in order to reach the appropriate conditions for ignition the relation $P_M < P_c$ has to be satisfied. In this context, the pressure of the pulse should be applied continuously as it is a function of the physical initial conditions related with the fuel seed, i.e. for given initial density $\rho_0 = 0.25\, g/cm^3$ and initial pressure $P_0 = 29.7Mb$, the above relation yields for the applied pressure the values $P(Mb) = 1.97, 3.087,\ 6.334,$ for post shock density equal to $\rho_M(g/cm^3) = 1, 1.4,$ and $2.4,$ respectively. Since the determination of the power and time of the shock pulse are very important quantities related with the maximum possible energy gain, the applied pressure must be a function of the pulse time. Therefore, to shape the adiabat we employ the DS approximation.

3. ADIABAT SHAPING THROUGH THE DS METHOD

The strong shock wave generated by the initial main pulse starts to decay after a certain time interval in which the pulse irradiates, and thus, the surface mass is an explicit function of the pulse irradiation time, $m_s = m_s(t)$. Employing the DS method we expand both the density, pressure and the velocity in powers of $\varepsilon(m_s(t))$, assuming the forms

$$\rho_N(\varepsilon) = \varepsilon^{\delta}\Phi(\varepsilon),\ P_N(\varepsilon) = \Phi^{\gamma}(\varepsilon), u_N(\varepsilon) = U(\varepsilon). \quad (18)$$

Here Φ and Uconsist of polynomial functions of ε, while δ is a constant the different values of which are determined from the solution of the equations of motion in Hugoniot conditions. In this case the adiabat S varies with time, following a simple power law through ε, as

$$S = \frac{P_M}{\rho_M^{\gamma}}\varepsilon^{-\gamma\delta}, \quad (19)$$

while the relation between m_s and ε has the explicit form

$$\dot{m}_s = \sqrt{\frac{\gamma-1}{2}\rho_M^{\gamma+1}\varepsilon^{\delta\gamma}}. \quad (20)$$

The above fina form of the corresponding ODE's must be solved for the coupled functions Φ and U together with the Hugoniot boundary conditions, which are obtained from the ones given in Eq. (16) as

$$\Phi(\varepsilon = 1) = 1, U(\varepsilon = 1) = \frac{2}{\gamma - 1}. \quad (22)$$

In order to solve approximately the system (21) we employ the following power law solutions with respect to ε

$$U(\varepsilon) = \sum_{i=0}^{k}\theta_i\varepsilon^i, \Phi(\varepsilon) = \sum_{i=0}^{k}\Delta_i\varepsilon^i, \quad (23)$$

the coefficients θ_i, and Δ_i, of which are to be determined from pertinent boundary conditions for different δ values. We have solved numerically the above system and calculated the values of the respective coefficients, up to the fourth order in $\varepsilon(k = 4)$, for five different assigned values of δ, in the interval $0.2 \leqslant \delta \leqslant 1.5$, in order to fully determine the solutions (23). These are presented in Table 1. We note that values $\delta > 1.5$ result to non physically plausible profiles of the pressure and density, and thus were not considered.

The specified profiles of Φ and U as functions of ε are plotted in Fig. 4 for the different assigned values of δ. It follows that the lower the value of δ, approaching zero, the functions Φ, U, and as a result, the fluid density and velocity converge to a straight line curve, thus, fixing the adiabat parameter value.

Table 1. The calculated values of the coefficients $\boldsymbol{\Delta_i, \theta_i}$ of the approximate solutions (23) for $\boldsymbol{\Phi(\varepsilon)}$ and $\boldsymbol{U(\varepsilon)}$ for $\boldsymbol{\delta = 0.2 - 1.5}$.

δ	$\Phi(\varepsilon)$					$U(\varepsilon)$				
	Δ_0	Δ_1	Δ_2	Δ_3	Δ_4	θ_0	θ_1	θ_2	θ_3	θ_4
0.2	1.025	-0.001	-0.026	0.005	0.003	3.27	-0.36	0.27	-0.27	0.1
0.6	1.1	-0.027	0.098	-0.055	-0.024	4.26	-3.46	-6.27	-6.8	2.74
1.0	1.2	-0.17	-0.13	-0.019	0.001	6.9	-18.6	46.1	-53.8	22.5
1.2	1.28	-0.38	0.32	-0.36	0.14	10	-41.9	114.4	-137.7	58.6
1.5	1.53	-1.81	4.39	-5.46	2.37	23.1	-164.7	506.4	-638.7	279

On account of the profiles (18) the system of ODE's obtained in (14) reduce into the following one

$$\frac{d\Phi^{\gamma}(\varepsilon)}{d\varepsilon} - \frac{\varepsilon(\gamma-1)}{2}\frac{dU(\varepsilon)}{d\varepsilon} = 0,$$
$$\varepsilon^{\delta}\frac{dU(\varepsilon)}{d\varepsilon} - \frac{1}{\Phi^2(\varepsilon)}\frac{d\Phi(\varepsilon)}{d\varepsilon} - \frac{\delta}{\Phi(\varepsilon)} = 0. \quad (21)$$

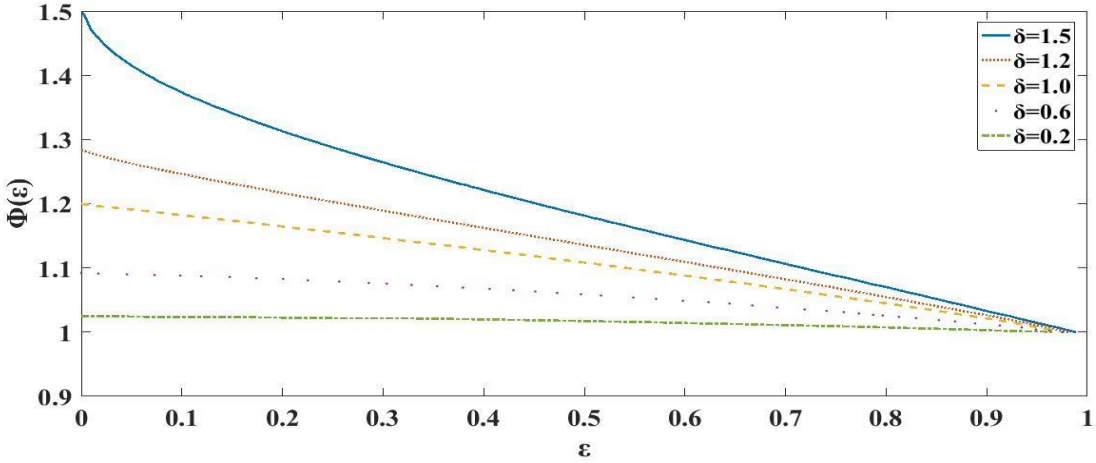

(a)

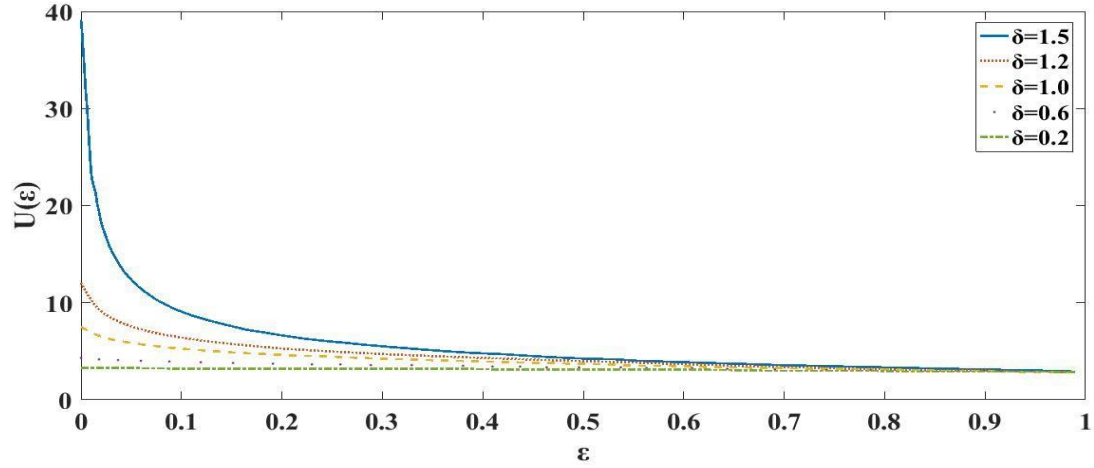

(b)

Figure 4. The behavior of the function $\Phi(\varepsilon)$ (a) and $U(\varepsilon)$ (b) for the different δ values assigned in Table 1.

The trajectory of the shock for each δ is obtained by a means of integration of the shock velocity equation (10), as

$$m_s(t) = \left\{\left(\frac{\delta\gamma}{2}+1\right)\sqrt{\frac{\gamma-1}{2}\rho_M^{\gamma+1}m^{\delta\gamma/2}t}\right\}^{\frac{2}{\delta\gamma+2}} \qquad (24)$$

leading to a respective relationship for the applied pressure, on account of the Hugoniot conditions, of the form

$$P(m=0,t) = \left(\frac{2}{\delta\gamma+2}\right)^{\delta\gamma/(\delta\gamma+2)} t^{-\delta\gamma/(\delta\gamma+2)} \times \qquad (25)$$

$$\times\left(\sqrt{\frac{\gamma-1}{2}\rho_M^{\gamma+1}m^{\delta\gamma/2}}\right)^{\frac{2}{\delta\gamma+2}} \int_0^1 u d\varepsilon.$$

From Eq. (25) it follows that the applied pressure is proportional to $t^{-\frac{\delta\gamma}{\delta\gamma+2}}$, and thus decays with time, this decay being enhanced as the value of the parameter δ enlarges. Based on the DS method employed, a step by step decrease in the post shock pressure P_M requires an increase in the pulse radiation time, once the intensity of the laser is lowered and thus, the applied pressure is decreased. The laser intensity, $I_L(PW/cm^2)$, relates to the applied pressure, $P(Mb)$, through (steady ablation theory)

$$P \simeq 40\left(\frac{I_L}{\lambda}\right)^{2/3}, \qquad (26)$$

where λ denotes the wavelength.

In order to shape the adiabat and calculate the adiabat parameter value, in respect to the most efficient process as concerns energy gaining and stability, related with the optimum laser power and radiation time, we solve numerically the system (21)-(22) to acquire the explicit expressions for U and Φin (23). Then, on account of these solutions we obtain the profiles of the pressure and

density through (18) and (25), as well as the laser intensity required to induce the pressure though (26).
We consider a fuel target of initial density $0.25 \leq \rho_0 \leq 0.6(g/cm^3)$, thickness $d = 100\mu m$, and inner thickness of the layer equal to $85\mu m$, in which a pulse created by a short wavelength $\lambda = 0.35\mu m$ is applied, in order to estimate the adiabat shaping. We find that the value $\delta = 1.2$ results to a nearly zero applied pressure, for which the laser intensity is negligible, and therefore, we reduce our analysis to values $\delta < 1.2$. For $\delta = 1$,0.6, and 0.2, we calculate the laser intensity needed to generate the pressure of 28, 24, 12, and 4 Mb, respectively, for different prepulse irradiation time. In specific, for three different density and pressure states for the aforementioned fuel, in which $\rho_0 = 0.25, 0.35, 0.6\, g/cm^3$and the post shock pressure is decreased from 20 Mb to 15 Mb to 10 Mb, we calculate the minimum adiabat parameter, as follows.
First state: In this state the values of the initial and the post shock densities were assigned as $\rho_0 = 0.25\, g/cm^3$ and $\rho_M = 1\, g/cm^{3,}$ respectively. Note that the post shock density is found from relation (8). The obtained intensity, radiation time and adiabat parameter values for each δ, are presented in Table 2.

Table 2. Estimated values of applied pressure, laser intensity, time and adiabat parameter for the state $\boldsymbol{\rho_M = 1\, g/cm^{3,}\, \rho_0 = 0.25\, g/cm^3}$.

Applied pressure (Mb)	4	12	24	28
Laser intensity (PW/cm^2)	0.09	0.469	1.33	1.67
Time (ps)for $\delta = 1$	2.46	0.735	0.343	0.289
Time (ps)for $\delta = 0.6$	360	69.3	24.5	19.5
Time (ps)for $\delta = 0.2$	4.410^5	9413	832	485
Adiabat parameter for $\delta = 1$	1.9	5.6	11.1	12.9
Adiabat parameter for $\delta = 0.6$	3	8.8	17.6	20.5
Adiabat parameter for $\delta = 0.2$	~ 100	~ 100	~ 100	~ 100

In this state, the density is fitted as a polynomial of the order two of ε:

$$\rho = -0.22\varepsilon^2 + 1.22\varepsilon - 0.0018, \qquad (27)$$

and the respective adiabat parameter for the different post shock pressures is shown in Fig. 5. It follows that the higher the value of the applied pressure and the exponent δ is, the lower adiabat parameter; that is, the optimum adiabat parameter in this state is calculated $\alpha = 1.9$, for $P = 4\, Mb$ and $\delta = 1$, achieved in time $t = 2.46\, ps$.
Second state: In this state the initial density is increased to the value $\rho_0 = 0.35\, g/cm^3$, resulting to a post-shock density $\rho_M = 1.4\, g/cm^3$; the calculated intensity, radiation time and adiabat parameter values for each $\delta$are shown in Table 3.
Furthermore, the density dependence in powers of ε for the employed δ values are obtained as

Table 3. Estimated values of applied pressure, laser intensity, time and adiabat parameter for the state $\boldsymbol{\rho_M = 1.4\, g/cm^{3,}\, \rho_0 = 0.35\, g/cm^3}$.

Applied pressure (Mb)	4	12	24	28
Laser intensity (PW/cm^2)	0.09	0.469	1.33	1.67
Time (ps)for $\delta = 1$	3.66	1.36	0.636	0.536
Time (ps)for $\delta = 0.6$	835.7	160.8	56.9	45.1
Time (ps)for $\delta = 0.2$	3.1310^5	6.710^4	5.910^3	3.410^3
Adiabat parameter for $\delta = 1$	1.1	3.2	6.3	7.4
Adiabat parameter for $\delta = 0.6$	1.7	5	10	11.3
Adiabat parameter for $\delta = 0.2$	~ 100	~ 100	~ 100	~ 100

$$\rho = \begin{cases} -0.31\varepsilon^2 + 1.7\varepsilon + 0.003, \delta = 1 \\ -0.95\varepsilon^2 + 2.16\varepsilon + 0.15, \delta = 0.6 \\ -1.21\varepsilon^2 + 1.893\varepsilon + 0.63, \delta = 0.2, \end{cases} \qquad (28)$$

and the corresponding adiabat parameter dependence in ε is shown in Fig. 6. We observe again that the lower adiabat parameter value is found for $\delta = 1$ and applied pressure equal to 4 Mb. In fact, reasonable values of α are obtained for $\delta = 0.6$ and applied pressure up to 12 Mb, these values however are achieved for longer time periods. The optimum adiabat parameter in this state is $\alpha = 1.1$, achieved for $t = 3.66\, ps$. This value is lower from the respective one obtained for the first state.
Third state: In this final state the values of the initial and post shock densities were further increased to $\rho_0 = 0.6\, g/cm^3$ and $\rho_M = 2.4\ g/cm^3$, respectively, leading to the following density profiles with respect to δ:

$$\rho = \begin{cases} -0.53\varepsilon^2 + 2.97\varepsilon + 0.0044, \delta = 1 \\ -1.64\varepsilon^2 + 3.7\varepsilon + 0.25, \delta = 0.6 \\ -2.07\varepsilon^2 + 3.253\varepsilon + 1.08, \delta = 0.2. \end{cases} \qquad (29)$$

Table 4. Estimated values of pressure, laser intensity, time and adiabat parameter for $\boldsymbol{\rho_M = 2.4\, g/cm^{3,}\, \rho_0 = 0.6\, g/cm^3}$.

Applied pressure (Mb)	4	12	24	28
Laser intensity (PW/cm^2)	0.09	0.469	1.33	1.67
Time (ps)for $\delta = 1$	12.25	3.66	1.7	1.44
Time (ps)for $\delta = 0.6$	3.210^3	618.8	218.8	173.6
Time (ps)for $\delta = 0.2$	7.210^7	1.510^6	1.410^5	8.0110^4
Adiabat parameter for $\delta = 1$	0.43	1.3	2.6	3
Adiabat parameter for $\delta = 0.6$	0.67	2	4	4.7
Adiabat parameter for $\delta = 0.2$	~ 100	~ 100	~ 100	~ 100

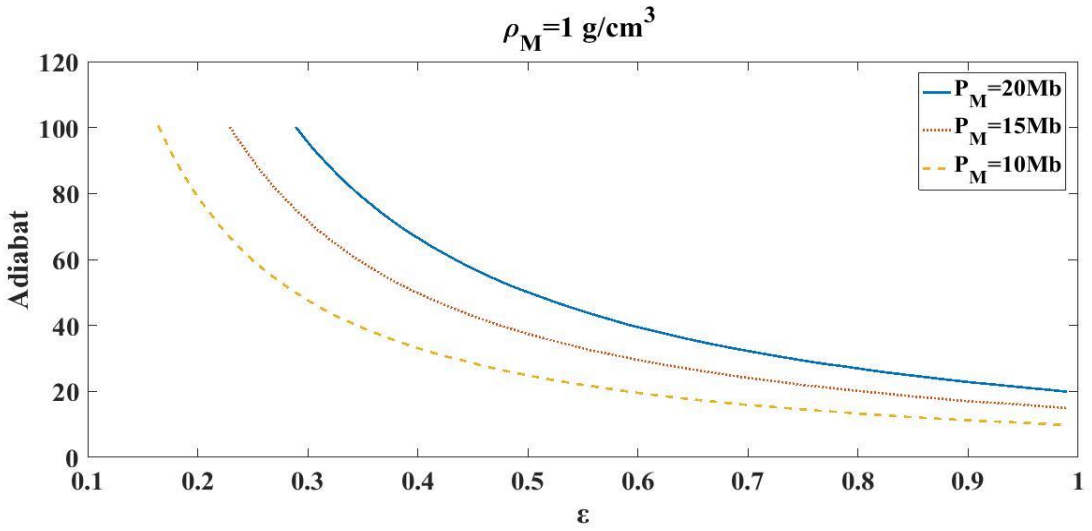

Figure 5. The adiabat parameter as a function of ε for the different post shock pressure values $P_M = 20\text{Mb}, 15\text{Mb}$ and 10 Mb in the first considered state.

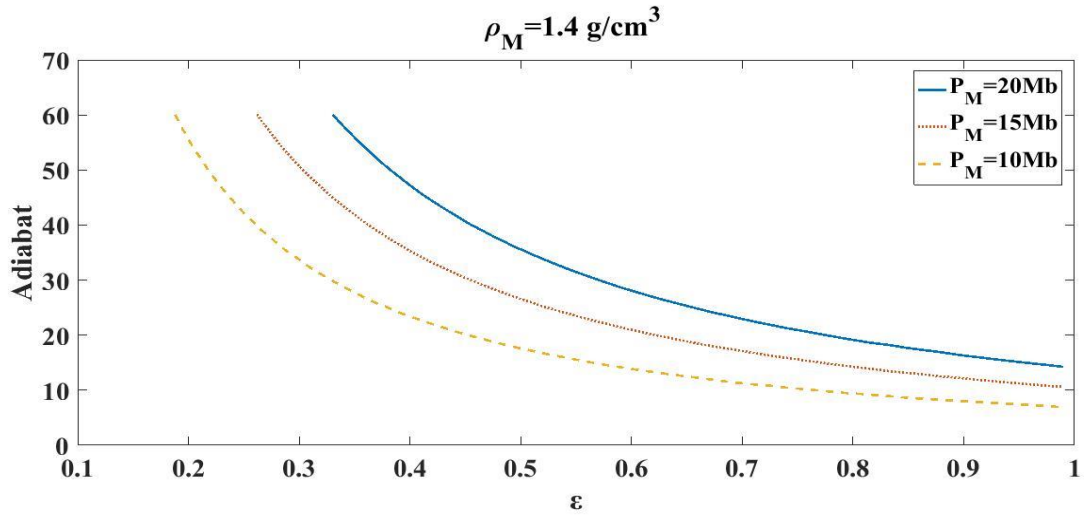

Figure 6. The adiabat parameter as a function of ε for the different post shock pressure values $P_M = 20\ Mb, 15\ Mb$ and 10 Mb related with the second state.

On account of the above equations we obtain the profile of the adiabat parameter shown in Fig. 7, for the values of applied pressure, laser intensity and radiation time calculated in table 4. We find that in this state the adiabat parameter is comparable to the one achieved in the previous state, but for a higher pressure; in specific, it is found that $12\ Mb$ is needed to set $a = 1.3$ for $t = 3.66\ ps$. Note that in this state the minimum adiabat parameter, found again for $P = 4\ Mb$ and $\delta = 1$, is significantly decreased to $\alpha = 0.43$ for $t = 12.25\ ps$. Thus, we conclude that the higher the initial density of the fuel is, the lower adiabat parameter.

4 CONCLUSIONS

Shaping the adiabat of the entropy during the implosions of ICF capsules plays an important role in the control and efficiency of the fuel targets in relation to a balance between energy gaining and stability. In the present paper we have considered the implosions of a two layer spherical shell, one of which consists of DT fuel and the other acts like a pusher, accelerated by the shock waves generated by a two-step pressure pulse. In specific, we have formulated the equations of motion together with the Hugoniot conditions for the related pressure and density profiles, and solved the resulting equations by employing the DS method since the applied pressure is a function of the time of the applied pulse. We investigated three different density for the target by increasing the initial density from $0.25\ g/cm^3$ to $0.35\ g/cm^3$ to $0.6\ g/cm^3$; in each of the states considered we numerically calculated the minimum adiabat parameter with respect to reasonable values for the applied pressure

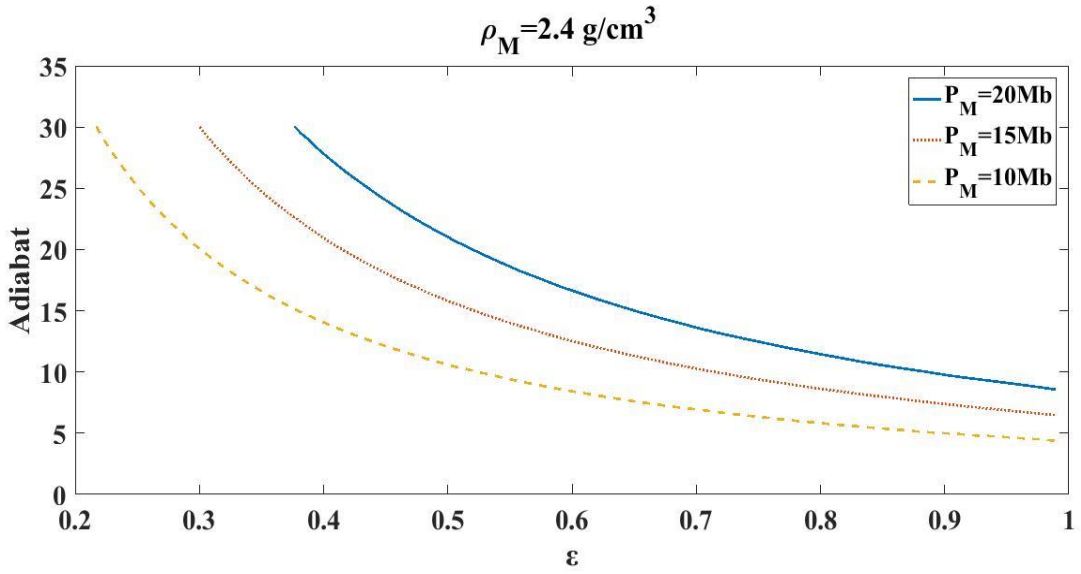

Figure 7. The adiabat parameter as a function of $\varepsilon$for the different post shock pressure values $P_M = 20\ Mb, 15\ Mb$ and 10 Mb related with the third state.

and the pulse radiation time. It follows that the lower the applied pressure and $\delta$is, the lower adiabat parameter, i.e. in all three states the minimum α was obtained for P = 4 Mb and δ = 1. Also we have found that the larger is the initial density of the fuel target, ρ_0, the lower the value of the minimum adiabat parameter.

In this respect we have found that the best adiabat parameter value obtained was $\alpha = 0.43$, acquired when the initial density of the fuel equals $\rho_0 = 0.6\ g/cm^3$ and the post shock density is equal to $\rho_M = 2.4\ g/cm^3$, for which the for pulse radiation time $t = 12.25\ ps$. The obtained adiabat parameter values are found to be comparable with the ones calculated in previous theoretical models and were achieved for relatively fast radiation times and low laser intensity required, herein. We conjecture that this may be beneficial as concerns the reduction of the growth rates of the driven instabilities in related ICF implosions.

DECLARATION OF ETHICAL STANDARDS

The author(s) of this article declare that the materials and methods used in this study do not require ethical committee permission and/or legal-special permission.

AUTHORS' CONTRIBUTIONS

Samira MOHAMMADKHANI: Performed the material identification and adjustment, data collection and analysis and wrote the first draft of the manuscript

Prof. Dr. Abbas Ghasemizad: Reviewed and commented on previous versions of the manuscript.

All authors read and approved the final manuscript.

CONFLICT OF INTEREST

There is no conflict of interest in this study.

REFERENCES

[1] Atzeni S. and Meyer-ter-Vehn J., "The Physics of Inertial Fusion: Beam Plasma Interaction, Hydrodynamics, Hot Dense Matter", International Series of Monographs on Physics, Clarendon, Oxford (2004).

[2] Lindl J. D., "Inertial Confinement Fusion : The Quest for Ignition and Energy Gain Using Indirect Drive", AIP Press, Springer, New York (1998).

[3] Craxton R. S., Anderson K. S., Boehly T. R., Goncharov V. N., Harding D. R., Knauer J. P., McCrory R. L., McKenty P. W., Meyerhofer D. D., Myatt J. F., Schmitt A. J., Sethian J. D., Short R. W., Skupsky S., Theobald W., Kruer W. L., Tanaka K., Betti R., Collins T. J. B., Delettrez J. A., Hu S. X., Marozas J. A., Maximov A. V., Michel D. T.,Radha P. B., Regan S. P., Sangster T. C., Seka W., Solodov A. A., Soures J. M., Stoeckl C. and Zuegel J. D., "Direct-drive inertial confinement fusion: A review", ***Physics of Plasmas***, 22(11): 110501 1-153 (2015).

[4] Campbell E. M., Goncharov V. N., Sangster T. C., Regan S. P., Radha P. B., Betti R., Myatt J. F., Froula D. H., Rosenberg M. J., Igumenshchev I. V., Seka W., Solodov A. A., Maximov A. V., Marozas J. A., Collins T. J. B., Turnbull D., Marshall F. J., Shvydky A., Knauer J. P., McCrory R. L., Sefkow A. B., Hohenberger M., Michel P. A., Chapman T., Masse L., Goyon C., Ross S., Bates J. W., Karasik M., Oh J., Weaver J., Schmitt A. J., Obenschain K., Reyes S. and Van Wonterghem B., "Laser-direct-drive program: Promise, challenge, and path forward ", ***Matter and Radiation at Extremes***,2(2): 37-54 (2017).

[5] Bodner S. E., Colombant D. G., Gardner J. H., Lehmberg R. H., Obenschain S. P., Phillips L., Schmitt A. J., Sethian J. D., McCrory R. L., Seka W., Charles P. V., Knauer J. P., Afeyan B. B. and Powell H. T., "Direct-drive laser fusion: Status and prospects", ***Physics of Plasmas***, 5(5): 1901-1918 (1998). [7] Aldabbagh L.B.Y., Egelioglu F. and lkan M., "Single and double pass solar air heaters with wire mesh as packing bed", ***Energy***, 35: 3783–3787, (2010).

[6] Lord Rayleigh, "Scientific Papers", Vol. II, Cambridge University Press, Cambridge (1900).

[7] Chandrasekhar S., "Hydrodynamic and Hydromagnetic Stability", Clarendon, Oxford (1961).

[8] Ghasemizad A., Zarringhalam H. and Gholamzadeh L., "The Investigation of Rayleigh-Taylor Instability Growth Rate in Inertial Confinement Fusion", ***J. Plasma Fusion Res. SERIES***, 8: 1234-1238 (2009).

[9] Bodner S. E., "Rayleigh-Taylor Instability and Laser-Pellet Fusion", ***Physical Review Letters***, 33(13): 761-764 (1974).

[10] Kilkenny J. D., Glendinning S. G., Haan S. W., Hammel B. A., Lindl J. D., Munro D., Remington B. A., Weber S. V., Knauer J. P. and Verdon C. P., "A review of the ablative stabilization of the Rayleigh-Taylor instability in regimes relevant to inertial confinement fusion", ***Physics of Plasmas***, 1(5): 1379-1389 (1994).

[11] Sanz J., "Self-consistent Analytical Model of the Rayleigh-Taylor Instability in InertialConfinement Fusion", ***Physical Review Letters***, 73(20): 2700-2703 (1994).

[12] Betti R., Goncharov V. N., McCrory R. L., Sorotokin P. and Verdon C. P., "Self- consistent stability analysis of ablation fronts in inertial confinement fusion", ***Physics of Plasmas***, 3(5): 2122-2128 (1996).

[13] Goncharov V. N., Knauer J. P., McKenty P. W., Radha P. B., Sangster T. C., Skupsky S., Betti R., McCrory R. L. and Meyerhofer D. D., "Improved performance of direct-drive inertial confinement fusion target designs with adiabat shaping using an intensity picket", ***Physics of Plasmas***, 10(5): 1906-1918 (2003).

[14] Anderson K. and Betti R., "Theory of laser-induced adiabat shaping in inertial fusion implosions: The decaying shock ", ***Physics of Plasmas***, 10(11): 4448-4462 (2003).

[15] Betti R., Anderson K., Knauer J., Collins T. J. B., McCrory R. L., McKenty P. W. and Skupsky S., " Theory of laser-induced adiabat shaping in inertial fusion implosions: The relaxation method ", ***Physics of Plasmas***, 12(4): 042703 1-18 (2005).

[16] Anderson K. and Betti R., "Laser-induced adiabat shaping by relaxation in inertial fusion implosions", ***Physics of Plasmas***, 11(1): 5-8 (2004).

[17] Betti R., Anderson K., Boehly T. R., Collins T. J. B., Craxton R. S., Delettrez J. A., Edgell D. H., Epstein R., Glebov V. Y., Goncharov V. N., Harding D. R., Keck R. L., Kelly J. H., Knauer J. P., Loucks S. J., Marozas J. A., Marshall F. J., Maximov A. V., Maywar D. N., McCrory R. L., McKenty P. W., Meyerhofer D. D., Myatt J., Radha P. B., Regan P. B., Ren C., Sangster T. C., Seka W., Skupsky S., Solodov A. A., Smalyuk V. A., Soures J. M., Stoeck C., Theobald W., Yaakobi B., Zhou C., Zuegel J. D., Frenge J. A., Li C. K., Petrasso R. D. and Seguin F. H., "Progress in hydrodynamics theory and experiments for direct-drive and fast ignition inertial confinement fusion", ***Plasma Physics and Controlled Fusion***, 48(12B): B153-B163 (2006).

[18] Baker K. L., Robey H. F., Milovich J. L., Jones O. S., Smalyuk V. A., Casey D. T., MacPhee A. G., Pak A., Celliers P. M., Clark D. S., Landen O. L., Peterson J. L., Berzk- Hopkins L. F., Weber C. R., Haan S. W., Doppner T. D., Dixit S., Giraldez E., Hamza A. V., Jancaitis K. S., Kroll J. J., Lafortune K. L., MacGowan B. J., Moody J. D., Nikroo A. and Widmayer C. C., "Adiabat-shaping in indirect drive inertial confinement fusion", ***Physics of Plasmas***, 22(5): 052702 1-9 (2015).

[19] Knauer J. P., Anderson K., Betti R., Collins T. J. B., Goncharov V. N., McKenty P. W., Meyerhofer D. D., Radha P. B., Regan S. P., Sangster T. C., Smalyuk V. A., Frenje J. A., Li C. K., Petrasso R. D. and Seguin F. H., "Improved target stability using picket pulses to increase and shape the ablator adiabat", ***Physics of Plasmas***, 12(5): 056306 1-6 (2005).

[20] Cheng B., Kwan T. J. T., Wang Y. M., Yi S. A., Batha S. H. and Wysocki F., "Ignition and pusher adiabat", ***Plasma Physics and Controlled Fusion***, 60(7): 074011 1-10 (2018).

[21] Piriz A. R. and Wouchuk J. G.,"Implosion of a two-layer shell driven by a shaped pressure pulse", ***Physics of Fluids B: Plasma Physics***, 3(10): 2889-2897 (1991).

[22] Collins T. J. B., Knauer J. P., Betti R., Boehly T. R., Delettrez J. A., Goncharov V. N., Meyerhofer D. D., McKenty P. W., Skupsky S. and Town R. P. J., "Reduction of the ablative Rayleigh-Taylor growth rate with Gaussian picket pulses", ***Physics of Plasmas***, 11(4): 1569 (2004).

[23] Zeldovich Y. B. and Raizer Y. P., "Physics of Shock Waves and High Temperature Hydrodynamic Phenomena", Wallace Hayes, Academic, New York (1967).

[24] Boehly T. R., Vianello E., Miller J. E., Craxton R. S., Collins T. J. B., Goncharov V. N., Igumenshchev I. V., Meyerhofer D. D., Hicks D. G., Celliers P. M. and Collins G. W., "Shock-timing experiments using double-pulse laser irradiation", ***Physics of Plasmas***, 13(5): 056303 1-7 (2006).

[25] Goncharov V. N., Gotchev O. V., Vianello E., Boehly T. R., Knauer J. P., McKenty P. W., Radha P. B., Regan S. P., Sangster T. C., Skupsky S., Smalyuk V. A., Betti R., McCrory R. L., Meyerhofer D. D. and Cherfils-Clerouin C., "Early stage of implosion in inertial confinement fusion: Shock timing and perturbation evolution", ***Physics of Plasmas***, 13(1): 012702 (2006).

[26] Whitham G. B., "Linear and Nonlinear Waves", Wiley, New York (1974).

[27] Vincenti W. G. and Kruger C. H., "Introduction to Physical Gas Dynamics", Wiley, New York (1965).

[28] Vold E. L., Joglekar A. S., Ortega M. I., Moll R., Fenn D. and Molvig K., "Plasma viscosity with mass transport in spherical inertial confinement fusion implosion simulations", ***Physics of Plasmas***, 22(11): 112708 1-11 (2015).